Structure of trigger factor binding domain in biologically homologous complex with eubacterial ribosome reveals its chaperone action

David Baram*, Erez Pyetan*, Assa Sittner, Tamar Auerbach-Nevo, Anat Bashan, and Ada Yonath†

Department of Structural Biology, The Weizmann Institute of Science, Rehovot 76100, Israel

Contributed by Ada Yonath, July 6, 2005

Trigger factor (TF), the first chaperone in eubacteria to encounter the emerging nascent chain, binds to the large ribosomal subunit in the vicinity of the protein exit tunnel opening and forms a sheltered folding space. Here, we present the 3.5-Å crystal structure of the physiological complex of the large ribosomal subunit from the eubacterium *Deinococcus radiodurans* with the N-terminal domain of TF (TFa) from the same organism. For anchoring, TFa exploits a small ribosomal surface area in the vicinity of proteins L23 and L29, by using its "signature motif" as well as additional structural elements. The molecular details of TFa interactions reveal that L23 is essential for the association of TF with the ribosome and may serve as a channel of communication with the nascent chain progressing in the tunnel. L29 appears to induce a conformational change in TFa, which results in the exposure of TFa hydrophobic patches to the opening of the ribosomal exit tunnel, thus increasing its affinity for hydrophobic segments of the emerging nascent polypeptide. This observation implies that, in addition to creating a protected folding space for the emerging nascent chain, TF association with the ribosome prevents aggregation by providing a competing hydrophobic environment and may be critical for attaining the functional conformation necessary for chaperone activity.

protein folding | nascent chain | ribosomal exit tunnel | ribosomal crystallography | *Deinococcus radiodurans*

The correct folding of newly synthesized proteins is a vital process in all kingdoms of life. Although protein sequences entail their unique folds (1), under cellular conditions nascent polypeptides emerging from the ribosomal tunnel are prone to aggregation and degradation, and thus require assistance of additional factors, called chaperones, which prevent misfolding during and after translation (2–6). In eubacteria, the folding of cytosol proteins is coordinated by three chaperone systems: the ribosome-associated trigger factor (TF), DnaK, and GroEL.

TF, the first chaperone to interact with the emerging nascent chain, is a 48-kDa modular protein composed of three domains: the N-terminal domain, which mediates association with the ribosome; the peptidylprolyl-*cis*/*trans*-isomerase (PPIase) domain; and the C-terminal domain (7). TF was shown to cooperate with the DnaK system, and the combined depletion of TF and DnaK (Δ*tig*Δ*dnaK* mutation) causes *Escherichia coli* cell death at >30°C as well as a massive aggregation of newly synthesized polypeptides (8).

TF binds to the large ribosomal subunit at 1:1 stoichiometry and occupies 90% of the ribosomes in the cytosol (9). It was shown to interact with ribosomal proteins L23 and L29, a prerequisite for its interaction with nascent chains and for its activity in the folding of newly synthesized proteins (10). A single mutation of the exposed glutamate-18 in L23 has been shown to prevent association of TF with the ribosome of *E. coli*, suggesting a specific binding site on the ribosome (11). High-resolution crystal structure of large ribosomal subunit from eubacterium *Deinococcus radiodurans* (12) revealed that protein L23 stretches from the vicinity of the ribosomal exit tunnel to the tunnel opening, implying a possible role in signal transduction and dynamic control (13).

Despite the abundance of biochemical data on the free and the bound TF, a single indisputable binding mode of the N-domain of TF (TFa) could not be reached, suggesting that TFa undergoes a significant conformational change upon association with the large ribosomal subunit (14). Some information about TF binding could be extracted from the crystal structure of a chimeric complex containing the large ribosomal subunit from the archaeon *Haloarcula marismortui* (H50S) with the eubacterial TFa from *E. coli* (15), called here 50S-EcTFa. This structure shows a substantial conformational change in the TFa binding loop containing the completely conserved "signature motif" (^{43}GFRXGXXP^{50}, *E. coli* numbers), as well as of a part of the helices surrounding it seen in the electron density map. However, because this complex revealed only a third of the TFa domain, and because the chaperone TF does not exist in the archaeal kingdom, the structure of the chimeric complex (9) provided only partial knowledge of the molecular detail of the interactions between TF and the ribosome.

Here, we present the 3.5-Å crystal structure of the physiological homologous complex of TFa from the eubacterium *D. radiodurans* bound to the large ribosomal subunit (D50S) from the same organism. This structure reveals the molecular details of the entire TFa bound to the bacterial ribosome, thus enabling analysis of its conformational changes and establishing a clearer understanding of its biological activity.

Materials and Methods

Strains, Plasmids, and Growth Conditions. Genomic DNA from *D. radiodurans* strain R1 (American Type Culture Collection no. 13939) was used for gene amplification. *E. coli* strain BL21 (Novagen) was used for protein overexpression. All strains were grown in Luria–Bertani (LB) medium; *E. coli* strains were grown at 37°C under antibiotic selection and *D. radiodurans* at 30°C.

Cloning. The primers 5′-GGAATTCCATATCGCAGAGCTGATCAGCAA-3′ and 5′-CGGGATCCTTATTACTCGAACGAGGCGTTG-3′ for PCR were designed to amplify the DNA fragment encoding for the N terminus (residues 1–151) of the gene *tig* of *D. radiodurans*. The PCR product was cloned into the pET-15b (Novagen) plasmid, which carries an N-terminal His-tag sequence followed by a thrombin site. The construct was inserted into the *E. coli* DH5α. The bacteria were grown, and the plasmids were purified by using a Plasmid midi kit (Qiagen).

Freely available online through the PNAS open access option.

Abbreviations: TF, trigger factor; TFa, N-terminal domain of trigger factor; D50S, large ribosomal subunit from *Deinococcus radiodurans*.

Data deposition: The atomic coordinates have been deposited in the Protein Data Bank, www.pdb.org (PDB ID code 2AAR).

*D.B. and E.P. contributed equally to this work.

†To whom correspondence should be addressed. E-mail: ada.yonath@weizmann.ac.il.

BIOCHEMISTRY

Protein Expression and Purification. The clone was inserted into *E. coli* BL21, and bacteria were then grown at 37°C until the culture reached an optical density of 0.6 at 560 nm. Protein expression was induced through addition of isopropyl 1-thio-β-D-galactopyranoside (Sigma) to a final concentration of 0.5 mM. Induction was followed by 2 h of incubation. The harvested bacteria were then disrupted by two cycles of French press at 8,000 psi (1 psi = 6.89 kPa). Purification of the His_6-tagged TFa was performed by using Ni–nitrilotriacetic acid affinity chromatography under native conditions (16), and the His-tag was removed by using thrombin. Size-exclusion FPLC was performed by using a Superdex 75 column (Amersham Pharmacia) equilibrated with 10 mM Hepes/10 mM $MgCl_2$/60 mM NH_4Cl for final purification.

Base and residue numbering is according to *D. radiodurans*. Ec attached to the right side of a number indicates *E. coli* numbering system.

Crystallization and Data Collection. Crystals of D50S were grown as described in ref. 17. The crystals were soaked in a harvesting solution containing 0.02 mM purified TFa for 10 h and finally heated to 37°C for an additional 50 min. After 20 min at room temperature (19°C), the crystals were briefly transferred into cryo-buffer (17) and shock-frozen in liquid nitrogen. Data were collected at 85 K by using synchrotron radiation at Beamline ID19 of the Structural Biology Center/Advanced Photon Source/Argonne National Laboratory (Chicago) and at Beamline ID14-4 of the European Synchrotron Radiation Facility/European Molecular Biology Laboratory (Grenoble). Data were recorded on Advanced Photon Source–charge-coupled device (Argonne National Laboratory) detectors and processed with HKL2000 (18) and the CCP4 package suite (19).

Structure Solution and Refinement. The native structure of D50S was refined against the structure factor amplitudes of the TF–50S complex by using rigid body refinement as implemented in CNS (20). For free *R* factor calculation, 5% of the data were omitted during refinement. The TF binding site was readily determined from sigmaa-weighted difference electron density maps. To enhance the detail, the difference maps were subjected to density modification using the CCP4 suite (19). The computed difference maps have unambiguously revealed the position of the TF binding domain as well as alterations in its environment. While tracing the structure of the bound TFa, the 2.3-Å crystal structure of the isolated N-terminal domain of TF (Protein Data Bank ID code 1OMS; ref. 14) served as a reference. Restraint minimization was carried out by using CNS (20). The resulting coordinates have been deposited at the Protein Data Bank (ID code 2AAR).

Results

Crystals of D50S in complex with the entire N-terminal binding domain of TF (also from *D. radiodurans*), yielded 3.5-Å resolution structures (Table 1). Unbiased Fourier difference maps revealed clear electron density for the entire TFa domain, and hence, enabled an unambiguous determination of its ribosome-bound structure (Figs. 1 and 2).

In general, the TFa bound structure accords with the previously determined tertiary folds of TF N-terminal domain (14, 15, 21). The signature motif (^{41}GFRXGXXP^{48}) is part of a loop, L1, surrounded by three α-helices (A1, A2, and A3), of which A2 and A3 are connected sequentially and appear together like a long broken α helix. The C terminus of A1 and the N terminus of A3 connect to an antiparallel β-structure (Fig. 2*a*).

The high quality of the electron density map (Fig. 2*b*) at TFa binding site and up to 35 Å away from its anchor point revealed the details of TFa contacts with ribosomal proteins L23 and L29, as well as demonstrated the orientation and conformation of helices A1, A2, and A3 (Fig. 2*a*). The N terminus of helix A1 seems partially disrupted because of its proximity to a neighboring ribosomal particle. Farther from the ribosome, the electron density map for TFa is less well defined. Yet, the two β turns and the N-terminal strand of the β-structure are unambiguously determined, enabling straightforward tracing of the α carbons of the entire β region, based on the previously published structures of this domain (14, 21).

Despite the similarity of the ribosome-bound TFa structure to crystal structures of the unbound domain, its overall conformation appears to be altered in a manner that clarifies its chaperone activity (Fig. 3*a*). In comparison with the unbound state (14, 15, 21), the binding region of TFa on the ribosome displays a rigid, well defined conformation, resembling that observed in the H50S–EcTFa complex. Helix A1 and helices A2 and A3, which in some structures appear as a single helix kinked at Gly-57 (Gly-59Ec) but not broken, are drawn 6 Å apart in the ribosome-bound structure in contrast to their being "wrapped on one another" in unbound TFa (14, 15, 21). Also, the β-sheet is not tightly packed with helix A3, as observed in all structures of unbound TFa. Because the interactions of helix A3 with helix A1 and with the β sheet are mainly hydrophobic in all structures of the unbound domain, and because these regions are buried in the unbound state, the separation between these structural features in the ribosome-bound structure increases the surface area of the exposed hydrophobic regions facing the ribosomal exit tunnel (Fig. 3 *b–d*).

The TF signature motif and its extension (the "extended signature motif"), including Lys-50 (Asn-52Ec) and the highly conserved Arg-55, interact with ribosomal proteins L23 and L29. TFa interacts with two separate exposed regions of the globular domain of protein L23: (*i*) residues Ile-12, Ser-13, and Glu-14 (Glu-18Ec) and (*ii*) C-terminal residues Ala-92, Gly-93, and Gln-94. It also interacts with a single exposed region of L29 (residues Ala-32, Ala-33, and Ala-34) (Fig. 4). Tangential interactions of TFa with the 23S rRNA include residues G1350, U1329, and G1330 of helix 50 and residue A1405 of helix 53.

The interactions of TFa signature motif residues Gly-41, Phe-42, and Arg-43 with L23 are rather similar to those identified in H50S–EcTFa (15). These residues are involved in extensive hydrophobic interactions with Ile-12, Ser-13, and Glu-14 of L23. Biochemical studies have shown that Glu-18Ec (Glu-14 in *D. radiodurans*) of L23 is essential for TF binding in *E. coli* (11). Consistently, we found that *D. radiodurans* Glu-14 of L23 offers two possible hydrogen bonds with Arg-45 of TFa, one with the backbone nitrogen and another with its N1.

Although hardly investigated previously, the structure of D50S–TFa complex reveals substantial contacts between loop L1 of TFa and the C terminus of L23. In the complex D50S–TFa, the latter appears to be somewhat more rigid than in the native

Table 1. Crystallographic data

Space group	*I*222
Wavelength, Å	0.97934
Unit cell parameters, Å	a = 169.4, b = 407, c = 692.7
Resolution range, Å	20–3.5 (3.62–3.5)
Unique reflections	289,641
Completeness, %	100 (100)
Redundancy	12.2 (9.5)
R_{sym} (%)	16.3 (71.8)
$\langle I\rangle/\langle\sigma(I)\rangle$	9.8 (1.5)
R, %	25.3
R_{free}, %	32.1
Bond distance rms, Å	0.008
Bond angles rms, °	1.4

Numbers in parentheses refer to the highest-resolution shell (3.62–3.5 Å).

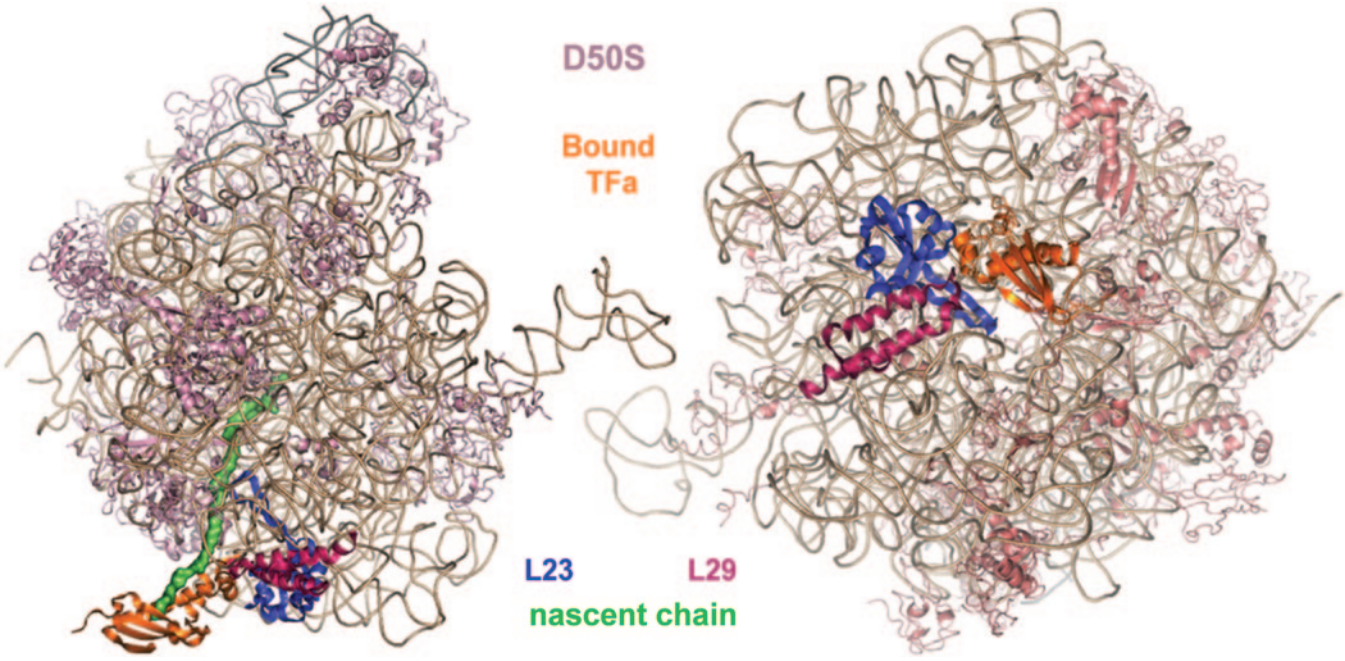

Fig. 1. The structure of TFa in complex with D50S. (*Left*) A side view of the large ribosomal subunit of *D. radiodurans* (represented by purple-brown RNA backbone and purple-pink ribosomal proteins main chains) with the bound TFa (orange) on a modeled (as in ref. 13) polypeptide chain (green surface). Ribosomal proteins L29 and L23 are highlighted in magenta and blue, respectively. (*Right*) A view into the ribosomal tunnel. Colors the same as in *Left*. Note the elongated loop of L23, a unique eubacterial feature, which reaches the interior of the tunnel, to a location allowing its interaction with the emerging nascent chain (in *Left*).

D50S structure (12) and exhibits a substantial conformational difference from that of the chimeric complex H50S–EcTFa. The most significant interaction in this region of the homologous complex D50S–TFa is a hydrogen bond between Lys-50 (Asn-52Ec) of TFa and the backbone carbonyl oxygen of Ala-92 of L23, an interaction not observed in the H50S–EcTFa complex. Residue Lys-50 of TFa is further engaged in hydrophobic interactions with Gly-93 and Gln-94 of L23.

Altogether, these interactions involve backbone atoms in the C terminus of L23, thus not depending on its level of conservation. Still, the H50S–EcTFa complex failed to detect a considerable amount of contacts in this region, possibly because of major differences between archaeal and bacterial L23 (13). In view of the observed differences, as well as the fact that TF does not exist in archaea, it is conceivable that these interactions play an important role in TFa chaperone's activity, which could not be revealed by an investigation of its nonphysiological association with the archaeal ribosome.

The contacts of ribosomal protein L29 with the C terminus of TFa helix A2 appear to have a substantial effect on the overall conformation of the bound TFa. The highly conserved TFa residue Arg-55 (Arg-57Ec) shares a hydrogen bond with the backbone carbonyl oxygen of Ala-32 of L29. Moreover, both Asn-54 and Arg-55 of TFa display hydrophobic interactions with Ala-32, Ala-33, and Ala-34 of L29. Only 15% of the buried surface area of the TFa–D50S complex results from its contacts with L29, consistent with biochemical evidence for its low contribution to TF association with the ribosome (11). Yet, these interactions with L29 could explain the 90° break in the A2–A3 structure around the conserved TFa Gly-57, which pulls helix A3 away from helix A1 and the β-structure, and results in the exposure of the hydrophobic patches. Noteworthy, these contacts do not exist in the H50S–EcTFa complex (15), possibly because of the disorder of helix A2 observed after a single α-turn.

Fig. 2. The crystallographic structure of bound TFa. (*a*) Structure of TFa upon association with the ribosome. (*b*) An unbiased $2F_o - F_c$ electron density map around helix A1, contoured at 1.5σ.

The interactions of TFa with helices 50 and 53 of the 23S rRNA appear to stabilize the binding conformation of its anchor by attaching the N terminus of the signature motif to the ribosome. The conserved TFa residue Gly-41 offers two possible hydrogen bonds with the backbone sugars of G1350 and G1351 of helix 50. Furthermore, hydrophobic interactions were detected between Arg-43 of TFa and A1405 of helix 53. Similar contacts appear in the H50S–EcTFa (15).

Overall, TFa extended signature motif is seen to interact with a compact region of the large ribosomal subunit at a triple junction between domain III of the 23S rRNA and ribosomal proteins L23 and L29. Glu-14 (Glu-18Ec) of L23, which was shown to be necessary and crucial for the association of TF with ribosome, lies at the center of this region, suggesting a possible role in TF recognition. The signature motif docked on Glu-14 of L23 serves as the central anchor on the ribosome, whereas the interactions with domain III of the 23S rRNA on one side, and those with L29 and the C terminus end of L23 on the other side appear to stabilize the binding conformation of loop L1 and helix A2 and render its unique fold.

Discussion

TFa Conformational Rearrangements and Their Implications. The crystal structure of the entire TFa, in complex with the large

BIOCHEMISTRY

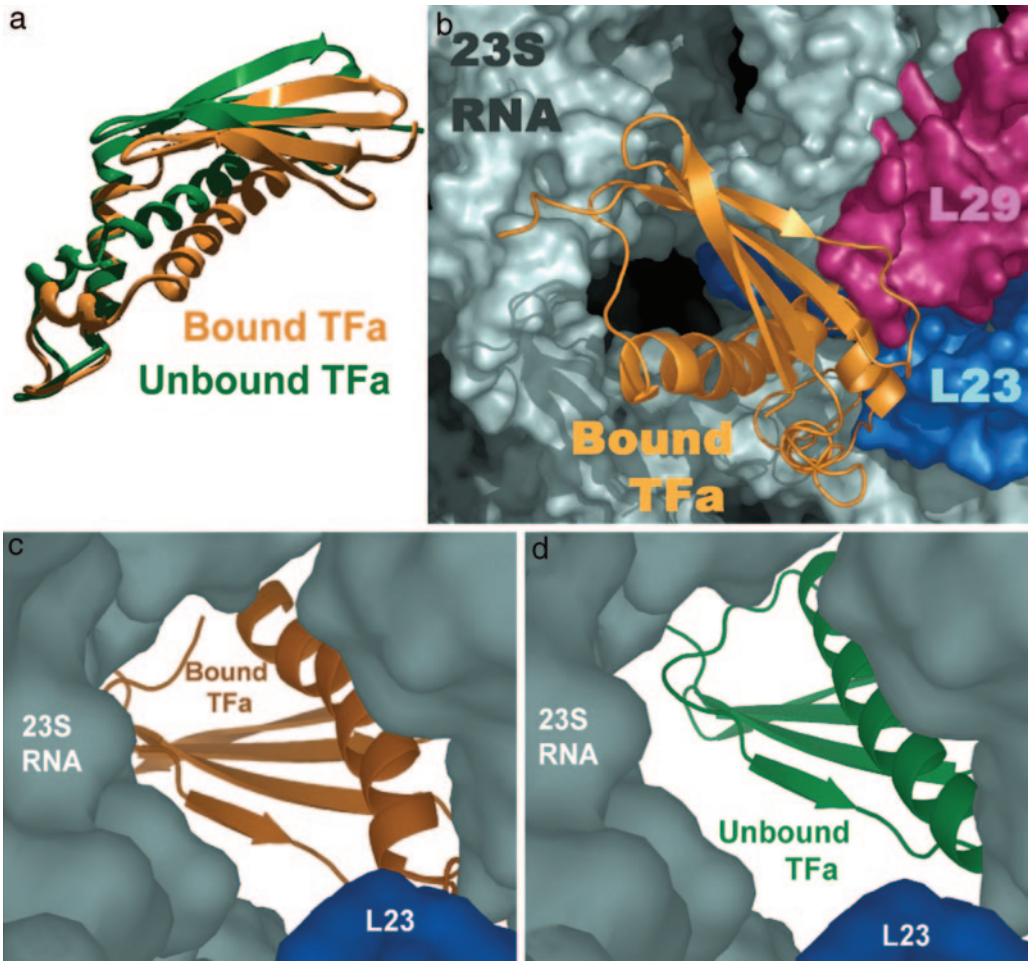

Fig. 3. Conformational rearrangements in TFa upon its association with the ribosome. In all images TFa is represented by its main chain, whereas the ribosomal components are shown as space-filling entities. Bound TFa, orange; unbound TFa, green; L23, blue; L29, magenta; 23S rRNA, light gray. (*a*) Superposition of the folds of unbound and bound TFa. To obtain this image, loop L1 and helix A1 of the unbound TFa (from PDB ID code 1OMS) were aligned with those of the bound TFa. (*b*) A view into the ribosomal tunnel highlighting the relative positioning of TFa, L23, and L29. (*c*) A view from the tunnel into the exposed hydrophobic pocket, created by the bound conformation of TFa. Note the β-sheet region, placed farthest from the actual tunnel opening (see Fig. 1 *Left*). (*d*) A hypothetical view of the structure that would been formed by TFa binding at its unbound conformation, indicating that the unbound conformation could not create a folding pocket. Tunnel orientation is as in *b*.

ribosomal subunit from eubacteria, reveals a significant conformational difference compared with its unbound structure, suggesting, in accord with previous biochemical results (14), that TFa adopts an altered structure upon its association with the ribosome. The previously reported native structures of TF and its N-terminal domain (14, 15, 21) display a substantial variability in the conformation of binding loop L1. Moreover, the 2.5-Å structure of unbound TF from *Vibrio cholerae* (21) does not show all of this loop's side chains, indicating its flexibility when not associated with the ribosome. In contrast, the electron density for this region in our difference Fourier maps and the resulting low *B* factors ensures rigidity of loop L1 in the bound state. Furthermore, the remarkable resemblance between the conformations of loop L1 in the physiological and in the chimeric H50S–EcTFa (15) complexes identifies a possible unique conformation of L1 when TF binds to the ribosome.

Of all unbound TF structures, the conformation of the *E. coli* L1 loop (14) bears the highest similarity to that of the bound

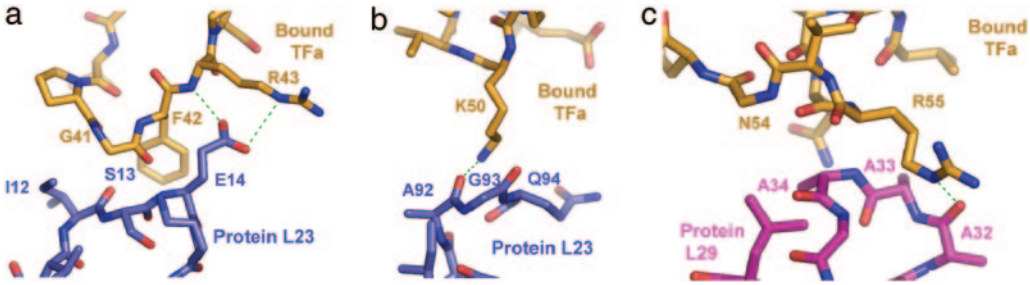

Fig. 4. Detailed molecular interactions of TFa (orange) with ribosomal proteins L23 (blue) (*a* and *b*) and L29 (magenta) (*c*).

state. Nevertheless, despite the very high homology between *E. coli* and *D. radiodurans* ribosomes and TFs, in the absence of a structure of a physiologically relevant complex of TF with the ribosome, this structure did not lead to the definition of the docking site for TFa on the 50S subunit (14). Indeed, superposing of the unbound TFa (14) on the location of the bound domain shows that, in the unbound structure, helix A2 is too far to interact with ribosomal proteins L23 and especially L29. Furthermore, it appears that the conformational change of the extended signature motif plays a key role in facilitating TFa docking on the 50S subunit. Consistently, a recent biochemical report has indicated that mutations and even deletion of the TF signature motif exert only a mild effect on TF function, compared with the complete deletion of the N-terminal domain (22). As association with the ribosome is a prerequisite for TF chaperone activity (23), the interactions of helix A2 with L29 and the C terminus of L23 seem to contribute significantly for TF binding.

It was shown that TF can be crosslinked to an emerging nascent chain when bound to the ribosome (24). Furthermore, TF is known to delay the folding and/or misfolding of nascent chains by recognizing hydrophobic regions in nascent polypeptides (25). The altered conformation of the TFa binding region forces helices A1 and A3 to lie further apart from one another, and consequently separates helix A3 from the β-sheets, thereby exposing a substantial hydrophobic pocket facing the opening of the ribosomal tunnel. The increase in the surface area of exposed hydrophobic regions seems to play a vital role in providing a supportive environment for aggregation prevention, thus facilitating, in turn, the correct folding of newly synthesized nascent chains. Consistently, biochemical studies have shown that the N-terminal domain of TF is necessary and sufficient to complement the synthetic lethality of $\Delta tig\Delta dnaK$ in cells lacking TF and DnaK, and to prevent protein aggregation *in vivo* (24).

Although we cannot exclude possible effects of crystal packing on TFa conformation, the low *B* factors and apparent rigidity of the TFa binding region compared with the high *B* factors of TFa in the vicinity of neighboring ribosomal components imply that the altered binding region, rather than the crystal packing, determines the overall structure. Consistently, when not associated with the ribosome, TFa does not display specific peptide binding in solution (26) and does not assist the refolding of denatured proteins (24). We therefore conclude that the observed TFa conformational change, which occurs upon association with the large ribosomal subunit and results in the exposure of a hydrophobic pocket, confers chaperone activity on TFa.

Fluorescence spectroscopy verified that the entire TF molecule exhibited comparable substrate specificity for peptides in solution, albeit at low affinity (26). Also, TF did not prevent aggregation of thermally unfolded proteins *in vitro* and did not complement the heat-sensitive phenotype of a $\Delta dnaK52$ mutant *in vivo* (23). These results indicate that the entire TF molecule requires ribosome association to create high local concentrations of nascent polypeptide substrates for productive interaction *in vivo*. As the structure of the entire TF was maintained to be relatively rigid (7), it is highly plausible that the exposure of the discussed hydrophobic pocket above the opening of the ribosomal tunnel exit is a critical factor in determining the chaperone's functional state.

Interaction with the Ribosome and Possible Role of L23. Within the entire binding region, the signature motif of TFa anchors on small exposed regions of ribosomal protein L23, in general agreement with the structure of the chimeric H50S–EcTFa complex (15). Importantly, in both chimeric and physiological homologous structures, all L23-interacting moieties belong to L23 globular domain, which is highly conserved in all kingdoms of life. The similarity of the TFa local interactions with both ribosomal systems is consistent with the high level of structural and sequence conservation of L23 interacting region with chaperones.

Despite the conservation of its globular region, protein L23 in eubacteria is significantly different from that of archaea and of eukaryotes, as it possesses a unique feature, a sizable elongated loop, which, in *D. radiodurans*, extends into the tunnel opening and can actively interact with the nascent protein passing through (12, 14). Our structure shows that TFa binds to two separate regions of L23 on both sides of the extended loop, thus linking the TF binding site with the ribosomal tunnel and enabling communication with the newly synthesized nascent chain. Specifically, the interaction of the progressing nascent polypeptide with the tip of the elongated loop of L23 may have a substantial impact on the binding of TF to the ribosome, consistent with its dissociation from the ribosome upon puromycin treatment (27).

In the TFa–ribosome bound structure, L23 of D50S exposes a sticky hydrophobic patch, located in the wall of the ribosomal tunnel and available for interactions with hydrophobic regions of the progressing nascent chain. Additionally, cotranslational folding of nascent polypeptides into secondary structures while still within the ribosomal tunnel has been detected in several cases (28–30). Upon their exit from the ribosome, such secondary structure elements may apply a substantial force to the tunnel wall (31) as well as to its opening. Specifically, the subjection of the elongated loop of protein L23, one of the main components at the tunnel opening, may affect, in turn, its interaction with TF.

The association of TF with the ribosome was asserted to form a molecular cradle for nascent proteins, which is large enough to accommodate globular protein domains up to a molecular mass of $\approx$15 kDa (15). In cases of multidomain bacterial proteins, such as β-galactosidase, additional TF molecules are recruited during translation, suggesting that, while maintaining contact with the elongated chain, the initially bound TF leaves the ribosomal docking site once sufficient sequence information is available for the generation of a folded core (25). However, because the dissociation of TF from the ribosome is a slow process (32), and protein domains vary in size and structure, a dynamic control of TF dissociation and reassociation during the translation of multidomain proteins is necessary to maintain efficient chaperone activity. Such a control mechanism could be mediated by L23, communicating information from the nascent polypeptide chain to the TF.

Conclusions. The 3.5-Å crystal structure of the physiologically meaningful complex of D50S with the binding domain of the TF from *D. radiodurans* elucidated critical aspects of this chaperone's activity. Upon association with the ribosome, TFa undergoes a conformational change, which exposes hydrophobic patches to the opening of the ribosomal tunnel, thereby facilitating its interactions with hydrophobic segments of the emerging nascent chain and preventing their aggregation. The ability of TFa to undergo rearrangements may also be linked to its functional activity in contributing an environment suitable for folding nucleation and, in turn, for controlling the progression of the folding process.

We thank all members of the ribosome group at the Weizmann Institute of Science. We especially thank Deborah Fass for fruitful discussions. X-ray diffraction data were collected at Beamline ID19 of the Structural Biology Center/Advanced Photon Source/Argonne National Laboratory and at Beamline ID14-4 of the European Synchrotron Radiation Facility/European Molecular Biology Laboratory. Support was provided by U.S. National Institutes of Health Grant GM34360 (to A.Y.), Human Frontier Science Program Organization Grant RGP 76/2003 (to A.Y.), and the Kimmelman Center for Macromolecular Assemblies. A.Y. holds the Helen and Martin Kimmel Professorial Chair.

1. Anfinsen, C. B. (1973) *Science* **181,** 223–230.
2. Rospert, S. (2004) *Curr. Biol.* **14,** R386–R388.
3. Frydman, J. (2001) *Annu. Rev. Biochem.* **70,** 603–647.
4. Hartl, F. U. & Hayer-Hartl, M. (2002) *Science* **295,** 1852–1858.
5. Thirumalai, D. & Lorimer, G. H. (2001) *Annu. Rev. Biophys. Biomol. Struct.* **30,** 245–269.
6. Gottesman, M. E. & Hendrickson, W. A. (2000) *Curr. Opin. Microbiol.* **3,** 197–202.
7. Maier, T., Ferbitz, L., Deuerling, E. & Ban, N. (2005) *Curr. Opin. Struct. Biol.* **15,** 204–212.
8. Deuerling, E., Schulze-Specking, A., Tomoyasu, T., Mogk, A. & Bukau, B. (1999) *Nature* **400,** 693–696.
9. Patzelt, H., Kramer, G., Rauch, T., Schonfeld, H. J., Bukau, B. & Deuerling, E. (2002) *Biol. Chem.* **383,** 1611–1619.
10. Blaha, G., Wilson, D. N., Stoller, G., Fischer, G., Willumeit, R. & Nierhaus, K. H. (2003) *J. Mol. Biol.* **326,** 887–897.
11. Kramer, G., Rauch, T., Rist, W., Vorderwulbecke, S., Patzelt, H., Schulze-Specking, A., Ban, N., Deuerling, E. & Bukau, B. (2002) *Nature* **419,** 171–174.
12. Harms, J., Schluenzen, F., Zarivach, R., Bashan, A., Gat, S., Agmon, I., Bartels, H., Franceschi, F. & Yonath, A. (2001) *Cell* **107,** 679–688.
13. Baram, D. & Yonath, A. (2005) *FEBS Lett.* **579,** 948–954.
14. Kristensen, O. & Gajhede, M. (2003) *Structure (Cambridge)* **11,** 1547–1556.
15. Ferbitz, L., Maier, T., Patzelt, H., Bukau, B., Deuerling, E. & Ban, N. (2004) *Nature* **431,** 590–596.
16. Qiagen (2000) *A Handbook for High Level Expression and Purification of 6xHis-tagged Proteins* (Qiagen, Valencia, CA).
17. Auerbach-Nevo, T., Zarivach, R., Peretz, M. & Yonath, A. (2005) *Acta Crystallogr. D* **61,** 713–719.
18. Otwinowski, Z. & Minor, W. (1997) *Methods Enzymol.* **276,** 307–326.
19. Bailey, S. (1994) *Acta Crystallogr. D* **50,** 760–763.
20. Brunger, A. T., Adams, P. D., Clore, G. M., DeLano, W. L., Gros, P., Grosse-Kunstleve, R. W., Jiang, J. S., Kuszewski, J., Nilges, M., Pannu, N. S., *et al.* (1998) *Acta Crystallogr. D* **54,** 905–921.
21. Ludlam, A. V., Moore, B. A. & Xu, Z. (2004) *Proc. Natl. Acad. Sci. USA* **101,** 13436–13441.
22. Genevaux, P., Keppel, F., Schwager, F., Langendijk-Genevaux, P. S., Hartl, F. U. & Georgopoulos, C. (2004) *EMBO Rep.* **5,** 195–200.
23. Schaffitzel, E., Rudiger, S., Bukau, B. & Deuerling, E. (2001) *Biol. Chem.* **382,** 1235–1243.
24. Kramer, G., Rutkowska, A., Wegrzyn, R. D., Patzelt, H., Kurz, T. A., Merz, F., Rauch, T., Vorderwulbecke, S., Deuerling, E. & Bukau, B. (2004) *J. Bacteriol.* **186,** 3777–3784.
25. Agashe, V. R., Guha, S., Chang, H. C., Genevaux, P., Hayer-Hartl, M., Stemp, M., Georgopoulos, C., Hartl, F. U. & Barral, J. M. (2004) *Cell* **117,** 199–209.
26. Patzelt, H., Rudiger, S., Brehmer, D., Kramer, G., Vorderwulbecke, S., Schaffitzel, E., Waitz, A., Hesterkamp, T., Dong, L., Schneider-Mergener, J., *et al.* (2001) *Proc. Natl. Acad. Sci. USA* **98,** 14244–14249.
27. Hesterkamp, T., Hauser, S., Lutcke, H. & Bukau, B. (1996) *Proc. Natl. Acad. Sci. USA* **93,** 4437–4441.
28. Woolhead, C. A., McCormick, P. J. & Johnson, A. E. (2004) *Cell* **116,** 725–736.
29. Eisenstein, M., Hardesty, B., Odom, O. W., Kudlicki, W., Kramer, G., Arad, T., Franceschi, F. & Yonath, A. (1994) in *Supramolecular Structure and Function*, ed. Pifat, G. (Balaban Press, Rehovot, Israel), Vol. 4, pp. 213–246.
30. Hardesty, B., Kudlicki, W., Odom, O. W., Zhang, T., McCarthy, D. & Kramer, G. (1995) *Biochem. Cell Biol.* **73,** 1199–1207.
31. Gilbert, R. J., Fucini, P., Connell, S., Fuller, S. D., Nierhaus, K. H., Robinson, C. V., Dobson, C. M. & Stuart, D. I. (2004) *Mol. Cell* **14,** 57–66.
32. Maier, R., Eckert, B., Scholz, C., Lilie, H. & Schmid, F. X. (2003) *J. Mol. Biol.* **326,** 585–592.